27

SELECTED PROBLEMS OF EMISSION INVENTORIES – GEOSTATISTICAL PERSPECTIVE

27.1 INTRODUCTION

Gridded emission inventories are key inputs to air quality models [34]. Spatial problems connected with a compilation of air emission inventories are frequently related to disaggregation [11, 27], or, in other words, an emission allocation [12]. Low-resolution emission inventories are usually carried out using the top-down approach dedicated to assess the estimates on the national or regional level [7] an then disaggregated, using various statistics known as the proxy data, e.g. population, population density, national fossil fuel consumption, indicators of the settlers' affluence (GDP per capita), or satellite observations of the phenomena such as: city lights intensity [24, 27, 38]. The disaggregation process makes possible to change the resolution of the emission inventory from the coarse to desired national emission grid [15]. Moreover, the practice of emission inventorying enables to combine various proxy data to create the 'optimal' spatial distributions of emission surrogates, related to unknown, but real spatial distributions of air emission fluxes [23].

However, the usage of GIS technologies [2, 14] can considerably facilitate the emission management process, including the possibility of estimate the high-resolution spatial air emission distribution applicable as an input for urban air quality research and policy [44]. Beside use of heterogenous emission surrogates allows to, obtain the uncertainty of the emission allocation, which is hard to assess, in another way. This problem usually causes various misinterpretations, e.g. impedes the perception of air emission related risks or reduces an effectiveness of mitigation and adaptation measures related to global change [37]. Using the geostatistical methods is applicable, and even awaited by scientific community in this matter [15, 21].

Population data is one of the most applicable proxies for spatial allocation of emission estimates, however, in this paper we would like to present usefulness of spatial techniques (such as indicator kriging) for the complex urban areas land cover (in particular urban infrastructure spatial distribution). The geostatistical methods are also recommended for changing resolution of selected calculated air emission estimates [9]. This spatial distribution is available as the product developed by the EEA [10]. The analysis is presented as the case study for the Katowice Urban Zone (KUZ), the central part of the Silesian Agglomeration, situated in southern part of Poland.

27.2 MATERIALS AND METHODS

The map density of urban development (called hereafter also as urban fabric, for brevity) is obtained from the EEA's Copernicus Land Monitoring Service [10]. For our analysis, we used the compilation of continuous and discontinuous urban fabric, due to complicated structure of urbanized areas in the KUZ. The study area showing density of urban development is presented in Fig. 27.1.

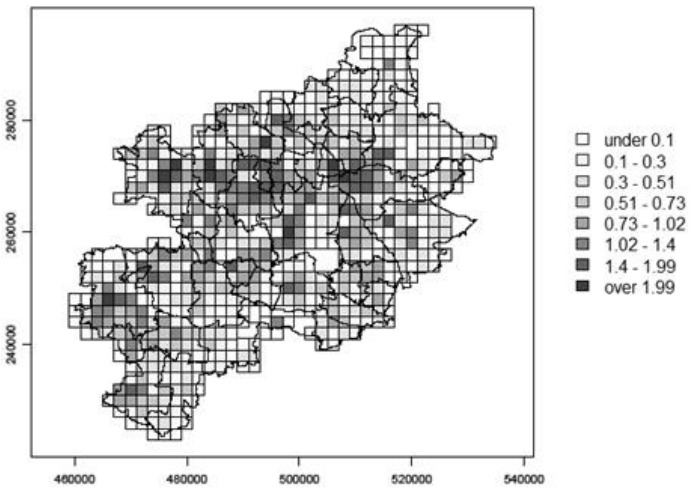

Fig. 27.1 Spatial distribution of urbanized areas density [km^2] aggregated in 2km × 2km grid

Source: [12]

The hot-spot of the density of built areas is located in the central-north part of analyzed region. Out of this area, the south of the region is more developed than the north side. The density of urbanized is extremely skewed (Fig. 27.2a). For this reason we applied in our analyses, the logarithmic (log10) transformation of density of urban development. From purely theoretical point of view, the potential disadvantages of the logarithmic transformation are: the occurrence of the 'edge effect' [35], and in some cases, impossibility of a back transforms application [36]. However, this kind of data transformation is widely applied for skewed data in practice [26, 45].

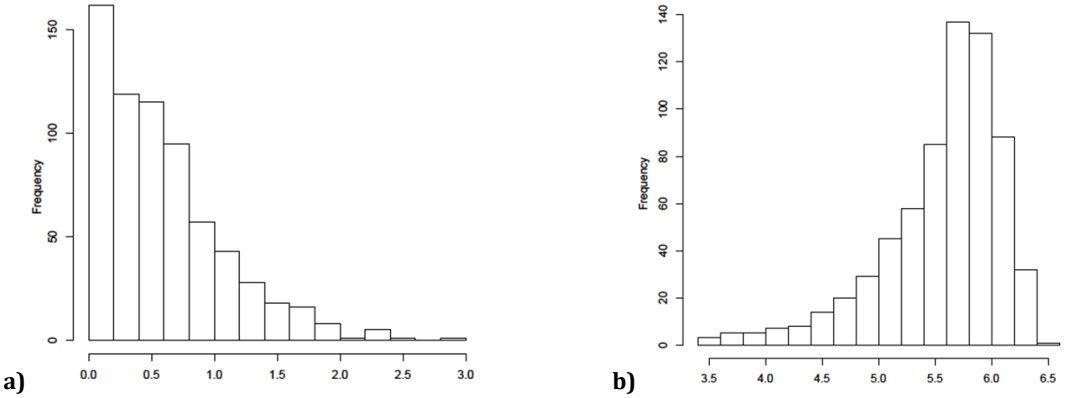

Fig. 27.2 Histogram for density urbanized areas

Source: own elaboraton

27.2.1 Spatial continuity analysis

For analysis of spatial continuity of the density of urban development, we applied the variogram analysis [5, 17, 35, 43], as following:

$$\gamma(h)=\frac{1}{2N(h)}\sum_{(i,j)h_{i,j}=h}[Z(x_i)-Z(x_i+h)]^2 \tag{27.1}$$

where: $\gamma(h)$ - semivariance for distance lag h;

h - distance [m];

$N(h)$ - number of grid pairs within distance h;

$Z(x_i), Z(x_i+h)$ - urbanized areas in points (grids) x_i and x_i+h.

We can also distinguish the nested variogram, which is linear combination of single variograms [6]:

$$\gamma(h)=\gamma_1(h)+\gamma_2(h)+...+\gamma_n(h) \tag{27.2}$$

27.2.2 Ordinary Kriging

Considering the built areas as point data focused in centroids of regular grid, the estimated at point $\hat{Z}(x_0)$ are weighted using surrounding data points according to spatial covariance [5, 17, 35, 43]:

$$\hat{Z}(x_0)=\sum_{i=1}^{N}\lambda_i z(x_i) \text{ and } \sum_{i=1}^{N}\lambda_i=1 \tag{27.3}$$

The Ordinary Kriging (OK) estimator is obtained by minimizing the variance over $\lambda_1,\lambda_2,...,\lambda_N$ using Lagrange multipliers method. That is:

$$\sigma_E^2=E\{[Z(x_0)-\hat{Z}(x_0))]^2\} \tag{27.4}$$

$$\mathbf{\Gamma}_O\boldsymbol{\lambda}_O=\boldsymbol{\gamma}_O \tag{27.5}$$

where: $\boldsymbol{\lambda}_O=(\lambda_1,\lambda_2,...,\lambda_N,m)'$ and $\boldsymbol{\gamma}_O=[\boldsymbol{\gamma}(x_1-x_0),...,\boldsymbol{\gamma}(x_N-x_0)]'$

$$\mathbf{\Gamma}_O=\begin{cases}\gamma(x_i-x_j) & \text{for } i=1,2,...,N,\ j=1,2,...,N\\ 1 & \text{for } i=N+1,\ j=1,2,...,N\\ 0 & \text{for } i=N+1,\ j=N+1\end{cases}$$

where: m is Lagrange multiplier, and matrix $\mathbf{\Gamma}_O$ is symmetric.

Minimized variance is called 'kriging variance':

$$\sigma_{OK}^2(x_0)=\sum_{i=1}^{N}\lambda_i\gamma(x_i-x_0)+m=\boldsymbol{\lambda}_O'\boldsymbol{\gamma}_O \tag{27.6}$$

27.2.3 Indicator Kriging

Indicator Kriging (IK) is a geostatistical technique used to approximate the conditional cumulative distribution function (ccdf) at each point of a grid based on the correlation structure of indicator transformed data points [18]. It proceeds the same way as the OK, but with the indicator random field $I(x,z_k)$ in place of Z_i and $\gamma_{I,z}(\cdot)$ in place of $\gamma(\cdot)$, under the conditions of second stationarity:

$$E[I(x,z)] \equiv F(z) \text{ for all } x \in D \text{ and all } z \in R$$
$$\text{var}\,[I(x,z) - I(x+h,z)] \equiv 2\gamma_{I,z}(h,z) \text{ for all } h \text{ and } z \in R,$$
$$I(x,z_k) = \begin{cases} 1 & \text{if } z \geq z_k, \\ 0 & \text{otherwise.} \end{cases} \tag{27.7}$$

The IK depicts the probability of exceedance of the value z_k [22]. IK is also a favored option for highly-skewed data sets, as it offers a practical way of treating the upper tail of the distribution which does not depend entirely on an arbitrary upper cut value [13].

27.3 RESULTS AND DISCUSSION

27.3.1 Spatial continuity analysis

Some of obtained anisotropic semivariograms tend to increase which results in negative correlations between variable values, for big distance lags h. We say then about the occurrence of the trend. There are three methods dedicated to dealing with the trend occurring in the semivariogram: fitting the trend surface, use a linear or power semivariogram model, or analysis of the semivariogram in the most 'trend-free' direction [4]. Only three from generated empirical models are trend-free, namely, the isotropic semivariogram (Fig. 27.3a) as well as semivariograms with anisotropy in the directions $\delta_1 = 0°$ (Fig. 27.3b, down-left) and $\delta_2 = 90°$ (Fig. 27.3b, up-left). The isotropic semivariogram was chosen for the further analysis, as the most reliable, on account of the maximal number of points taken into account.

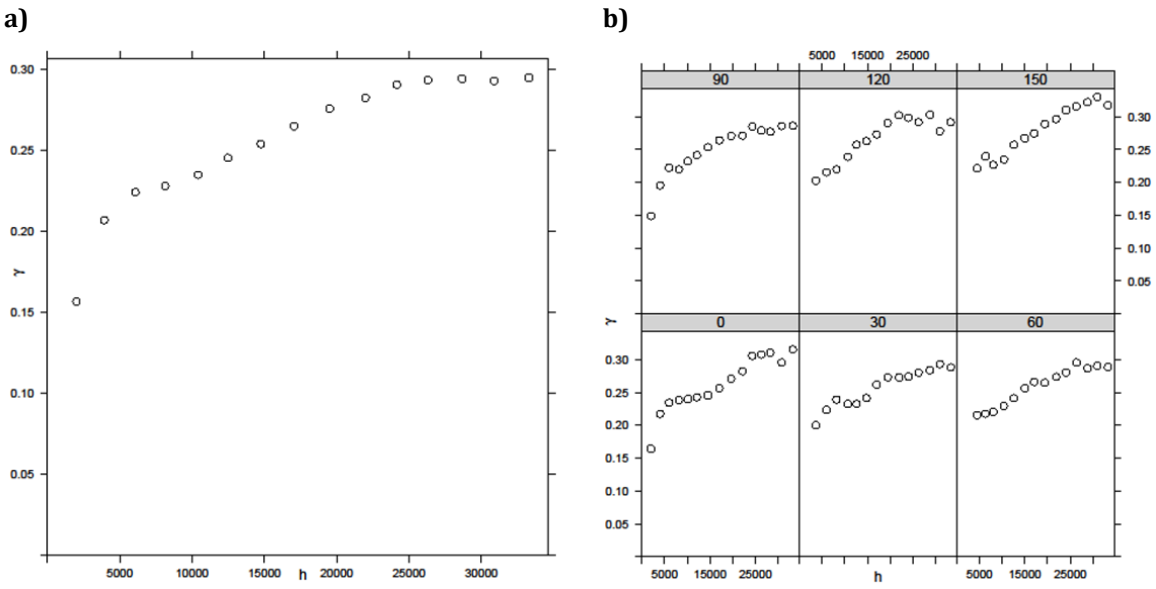

Fig. 27.3 Empirical semivariograms for logarithmized (log10) density of the urban development $\delta \in \{0°,30°,60°,90°,120°,150°\}$, h distance [m]; γ, semivariance [(log10 m²)²]

Source: own elaboration

For the empirical isotropic semivariogram (Fig. 27.3a), using models: spherical (27.8) and gaussian (27.9), we applied separately two nested structures. They are linear combinations of three (Fig. 27.4a) and two (Fig. 1.4b) nested structures respectively.

$$\gamma(h)=\begin{cases} c\cdot\left(\frac{3h}{2a}-\frac{1}{2}\cdot\left(\frac{h}{a}\right)^3\right) & \text{if } h\le a \\ c \text{ otherwise} \end{cases} \tag{27.8}$$

$$\gamma(h)=c\left(1-\exp\left(\frac{-3h^2}{a^2}\right)\right) \tag{27.9}$$

where: h - distance [m];
a - (practical) range and
c - sill.

Detailed parameters of the fitted theoretical models are given in Tab. 27.1.

Tab. 27.1 Parameters of the fitted nested models

Structure	Model	Sill $s\,[(\log_{10}\mathrm{m}^2)^2]$	Range $a\,[\mathrm{m}]$	*SSE*
1 (Fig. 27.4a)	Nugget effect	0.02	0.000	2.455·10-7
	Spherical	0.12	2.000	
	Spherical	0.08	5.500	
	Gaussian	0.07	16.500	
2 (Fig. 27.4b)	Nugget effect	0.09	0.000	2.686·10-9
	Spherical	0.13	5.214	
	Gaussian	0.09	19.339	

Source: own elaboration

The theoretical model is chosen by comparison the SSE (sum of squared errors), underlined in Tab. 27.1. Lower SSE value indicates the best fit [25].

Considered models for theoretical semivariograms are presented in the Fig. 27.4. The nested structures are added for the empirical semivariogram and marked with a thick line. Application of the nested models causes that the goodness of fit, expressed by the SSE value, quickly reaches the saturation point [30]. Moreover, the combination of the Gaussian and spherical model performs effectively over multiple lag distances [6].

However the guidelines does not suggest more than 2 variogram models incurporated in the nested structure [3], in our case the best fit consists of 3 variogram models (Fig. 27.4b).

27.3.2 Ordinary Kriging

OK is performed for the logarithmized (log10) density of urban development using variogram model having the lowest SSE value. Apart from the estimation and variance, we performed the cross validation of the results using the 'leave-one-out' (LOO) approach.

The LOO technique estimates (OK) the value in place x0 using the data created by removing the x0 from the original data set [1, 8, 16]. The result of the OK estimation and cross validation is presented in the Fig. 27.5 and 27.6.

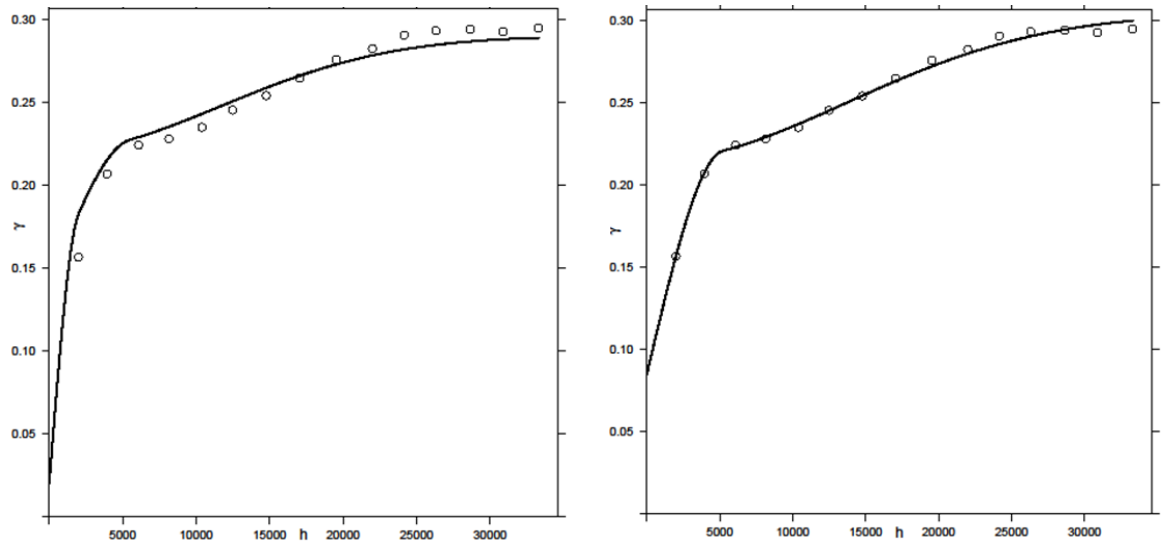

a) Fitted model: nugget effect + spherical1 + spherical2 + gaussian, Tab. 27.1, Structure 1

b) Fitted model: nugget effect + spherical + gaussian, Tab. 27.1, Structure 2

Fig. 27.4 Empirical variogram of the logarithmized (log_{10}) density of urban development and fitted models of the nested structures

Source: own elaboration, The same units as in Fig. 27.3

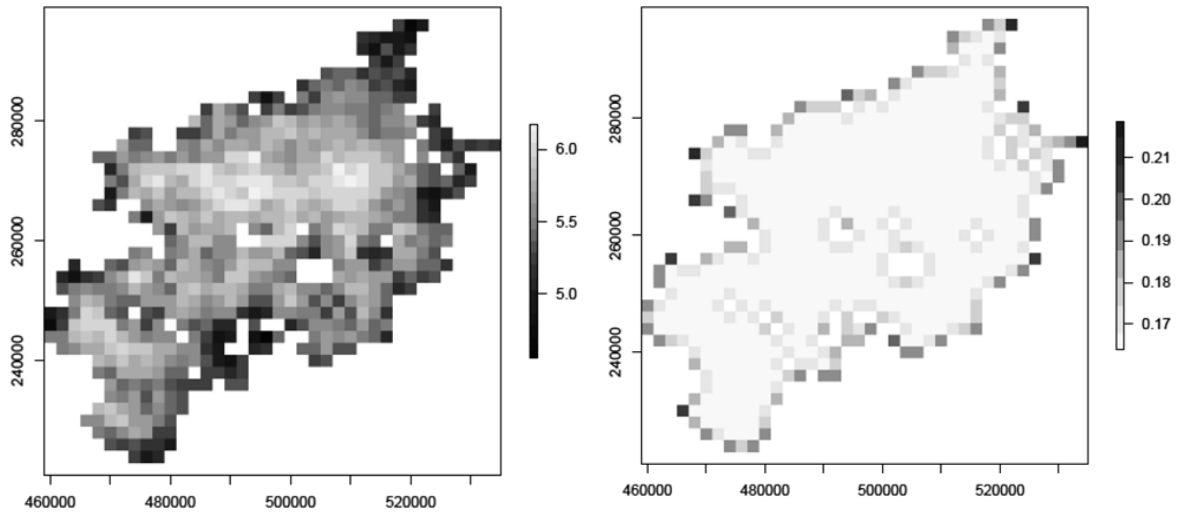

a) Estimation [log10 m²]

b) OK's variance [(log10 m²)²]

Fig. 27.5 Ordinary Kriging for the logarithmized density of urban development in the KUZ

Source: own elaboration

Analysis of the estimated values (Fig. 27.5a) and the OK's variance (Fig. 27.5b) indicates two drawbacks of the logarithmic transformation: smoothing tendency (Fig. 27.5a), and the edge effect (Fig. 27.5b, on the rim of the region).

Comparison the estimation (OK) performed for the complete data set (Fig. 27.5a) with the cross validation (Fig. 27.6a), indicates that the assumed spatial model (Fig. 27.4b) overestimates, primarily, lower values.

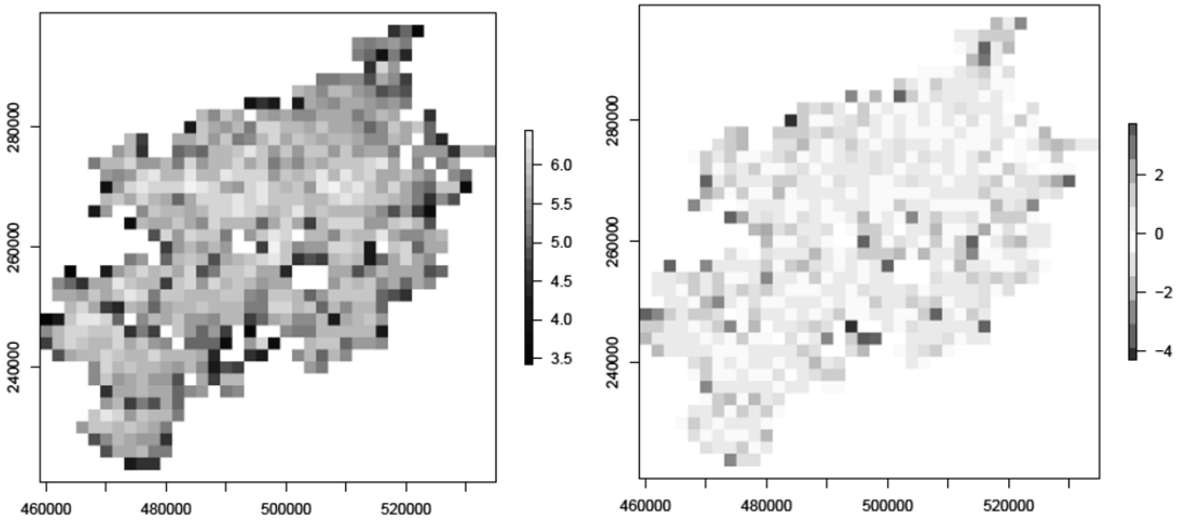

a) The results of cross validation [$\log_{10}$ m^2] **b) Z-score**

Fig. 27.6 Kriged logarithmized density of urban development in the KUZ

Source: own elaboration

The z-score, presented in the Fig. 27.6b, is the spatial distribution of standardized difference between the estimation (Fig. 27.5a) and the result of the cross validation (Fig. 27.6a) calculated using the OK's standard deviation.

27.3.3 Indicator Kriging

The Indicator Kriging [42] is introduced to assess the probability of exceedance of the particular percentiles of logarithmized built areas. For analysis are chosen percenTiles: 75th, 85th and 95th. Selected values are presented in Fig. 27.7a. Taking into consideration the current trends in emission inventories elaborated for air quality modeling, mainly emission mapping in 1km × 1km resolution [3, 29, 31, 33, 40, 46], we decided to distinguish built area of 1km^2 which is 25% of the single grid area (see Fig. 27.1). Because the value of 3rd quartile of logarithmized density of urban development is near to 6 (5.922), the analyzed initial percentiles are chosen basing on that value, as: 75th (5.92), 85th (6.04) and 95th (6.20) [log10 m^2]. From all chosen percentiles the value of the 85th one is the nearest to 6. Basing on that the final value is chosen.

Using the approach taking into account spatial continuity analysis, that is fitting the theoretical variogram model to the empirical one, we found the spherical model, as the most appropriate (Eq. 27.8). The fit is presented in Fig. 27.7b. Parameters of fitted theoretical model are: nugget effect, 0.08 [log10 m^2]; range: a = 7,385.9 [m]; sill: s = 0.1398 [log10 m^2]; SSE = $1.199 \cdot 10^{-8}$. The results of IK performance is presented in Fig. 27.8. The result of the IK's performance for $P\{z(x) \geq 6.04\} = 1$, where z(x) is logarithmized (log10) density of urban development is shown in the Fig. 27.8a. These areas coincide well with the, scheme of the Silesian Heating System infrastructure derived from [28, 32].

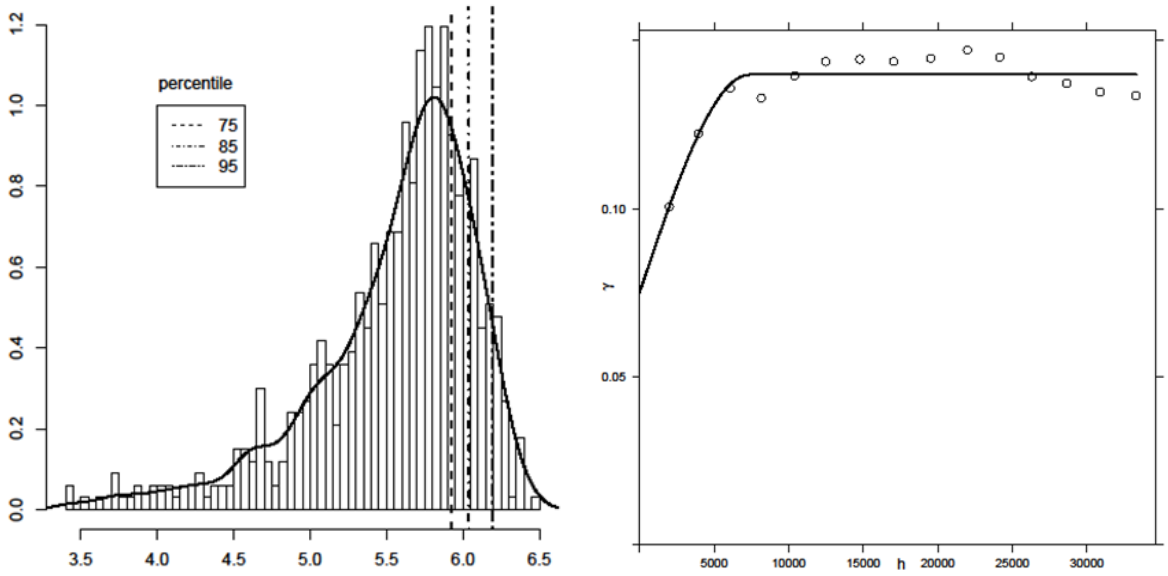

a) Selected percentiles of logarithmized density [log10 m²]

b) Theoretical variogram model for 85th percentile of density (units as in Fig 27.3)

Fig. 27.7 Urban development in the KUZ

Source: own elaboration

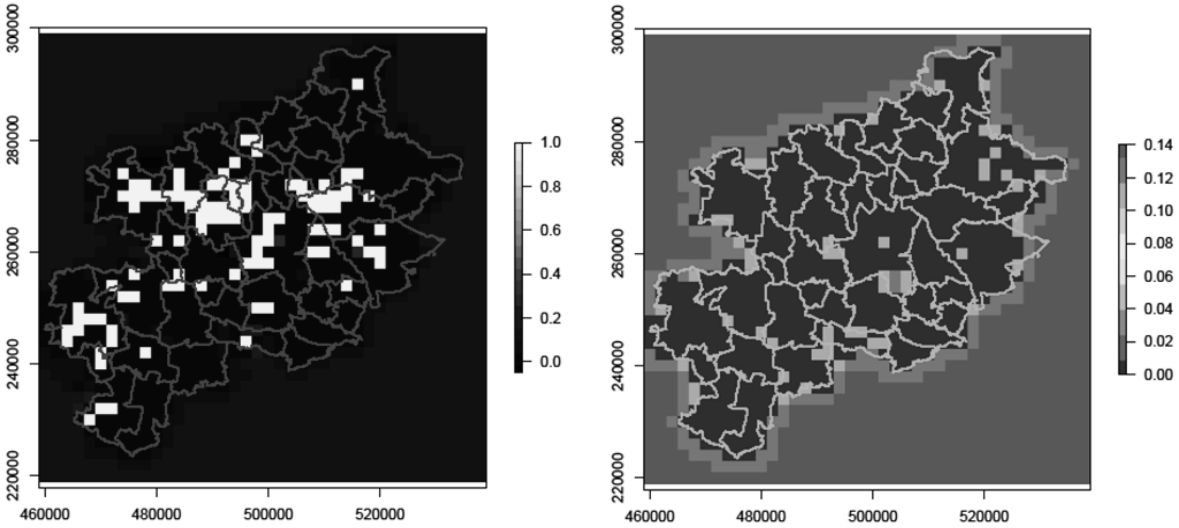

a) Estimation P{z(x) ≥ 6.04}

b) IK's variance [(log10 m²)²]

Fig. 27.8 IK for logarithmized density of urban development

Source: own elaboration

CONCLUSIONS

Our analysis presented in this paper applies a new approach to the spatial air emissions, disaggregation based on geostatistical techniques, namely, ordinary and indicator kriging combined with techniques of cross validation. The most important, practical finding is the geostatistically based specification of the links between the characteristic of built areas and the location of district heating infrastructure (Fig. 27.9).

The application of elaborated methodology can significantly facilitate the air emission disaggregation and estimation from small and scattered, emitting sources such as, e.g. domestic cooking or heating, which are considerably source of the 'low emission' [19, 20, 41].

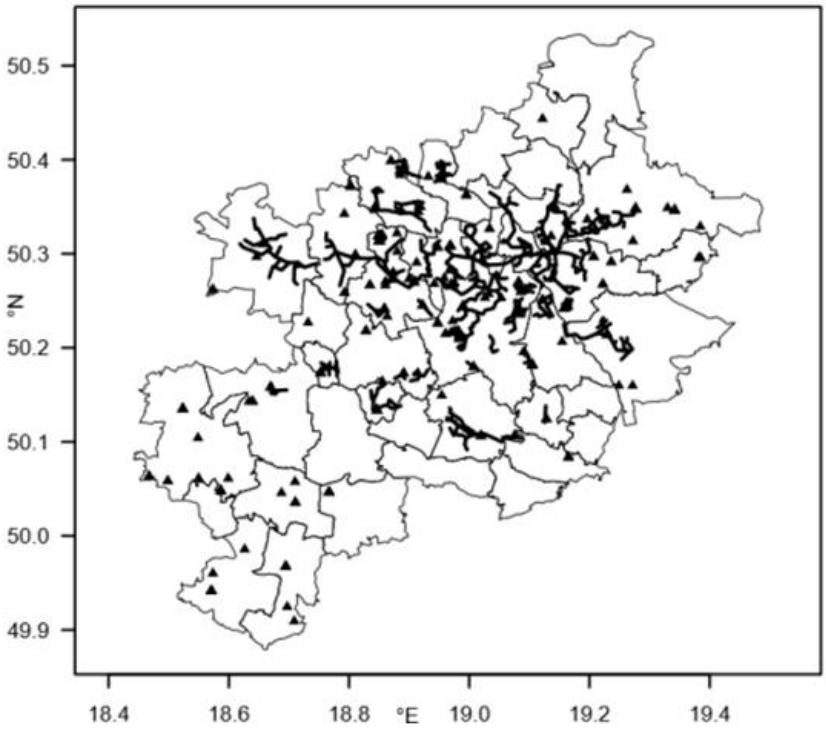

Fig. 27.9 The simplified scheme of the SHS infrastructure: triangles, plants; lines, main heating arteries

Source: own elaboration

Occurrence of infrastructure (as district heating system) considerably changes the emission split between the public power sector (power and energy plants) and small domestic combustion. The dwellers supplied with the heat and hot water from the district heating infrastructure do not use small, individual stoves. Due to this fact, the air emission mapping for small sources should take into account big district heating systems.

REFERENCES

1. M. Armstrong. Basic Linear Geostatistics. Springer, 1998, https://doi.org/10.1007-/978-3-642-58727-6.
2. S. Behera, M. Sharma, O. Dikshit, and S. Shukla. *Development of GIS-aided Emission Inventory of Air Pollutants for an Urban Environment*. InTech, 2011, pp. 279-294, available from: http://www.intechopen.com/books/advanced-air-pollution/development-of-gis-aided-emission-inventory-of-air-pollutants-for-an-urban-environment.

3. J. Bieser, A. Aulinger, V. Matthias, M. Quante, and P. Builtjes. „SMOKE for Europe – adaptation, modification and evaluation of a comprehensive emission model for Europe." Geoscientific Model Development, vol. 4, pp. 47-68, 2011, https://doi.-org/10.5194/gmd-4-47-2011.
4. G. Bohling. „Introduction to geostatistics and variogram analysis," 2005, http://people.ku.edu/~gbohling/cpe940/Variograms.pdf [Dostęp: 12.02.2017].
5. J.-P. Chilès and P. Delfiner. *Geostatistics. Modeling Spatial Uncertainty* 2nd edt. John Wiley & Sons, 2012.
6. S.-O. Chung, K. Sudduth, S. Drummond, and N. Kitchen. „Spatial Variability of Soil Properties using Nested Variograms at Multiple Scales." *Journal of Biosystems Engineering*, vol. 39, no. 4, p. 377-388, 2014, https://doi.org/10.5307/JBE.2014.39.-4.377 [Dostęp: 23.03.2017].
7. H. Denier van der Gon, S. Beevers, A. D'Allura, S. Finardi, C. Honoré, J. Kuenen, O. Perrussel, P. Radice, J. Theloke, M. Uzbasich, and A. Visschedijk. „Discrepancies Between Top-Down and Bottom-Up Emission Inventories of Megacities: The Causes and Relevance for Modeling Concentrations and Exposure," in Air Pollution Modeling and its Application XXI, D. Steyn and S. Trini Castelli, Eds. Dordrecht: Springer, 2011, p. 199-204, https://dx.doi.org/10.1007/978-94-007-1359-8_34.
8. C. Deutsch. *Geostatistical Reservoir Modeling.* Oxford: Oxford University Press, 2002.
9. EEA and EMEP LRTAP, EMEP/EEA air pollutant emission inventory guidebook 2016, 2016, https://doi.org/10.2800/247535 [Dostęp: 23.01.2017].
10. EEA, "CLC 2012," 2012, http://land.copernicus.eu/pan-european/corine-land-cover-/clc-2012 [Dostęp: 24.01.2017].
11. J. Ferreira, M. Guevara, J. Baldasano, O. Tchepel, M. Schaap, A. Miranda, and C. Borrego. „A comparative analysis of two highly spatially resolved European atmospheric emission inventories." Atmospheric Environment, vol. 75, pp. 43-57, 2013, https:-//doi.org/10.1016/j.atmosenv.2013.03.052 [Dostęp: 21.03.2017].
12. D. Gkatzoflias, G. Mellios, and Z. Samaras. „Development of a web GIS application for emissions inventory spatial allocation based on open source software tools." Computers & Geosciences, vol. 52, pp. 21-33, 2013, https://doi.org/10.1016/j.cageo.-2012.10.011 [Dostęp: 17.04.2017].
13. I. Glacken, P. Blackney. „A practitioners implementation of indicator kriging," Perth, Western Australia, 1998, 'Beyond Ordinary Kriging', Seminar October 30th, 1998. http://www.gaa.org.au/pdf/bok%20glacken.pdf [Dostęp: 19.05.2017].
14. J. Horabik-Pyzel and Z. Nahorski. „Integration of multi-source information in disaggregation of spatial emission data," 2015, 4th International Workshop on Uncertainties in Atmospheric Emissions Kraków, 7-9 October 2015. Available from: http://-www.ibspan.-waw.pl/unws2015/images/presentations/gridded_emissions/gridded_emissions_4.pdf [Dostęp: 13.05.2017].

15. J. Horabik-Pyzel and Z. Nahorski. „Uncertainty of Spatial Disaggregation Procedures: Conditional Autoregressive Versus Geostatistical Models." Proceedings of the Federated Conference on Computer Science and Information Systems, vol. 8, pp. 449-457, 2016, https://doi.org/10.15439/2016F539 [Dostęp: 02.04.2017].
16. E. Isaaks, R. Srivastava. *Applied Geostatistics*. New York: Oxford University Press, 1989.
17. A. Journel. *Fundamentals of Geostatistics in Five Lessons*. Washington DC: American Geophysical Union, 1989, vol. 8, https://www.nrc.gov/docs/ML0227/ML0227700-97.pdf [Dostęp: 12.03.217].
18. A. Journel. „Nonparametric estimation of spatial distributions." *Journal of the International Association for Mathematical Geology*, vol. 15, p. 445-468, 1983, https://doi.-org/10.1007/BF01031292 [Dostęp: 21.05.2017].
19. D. Kaleta. „State of Air Pollution in Silesia Province Including Low Emission Sources." *Architecture Civil Engineering Environment Journal*, vol. 7, no. 4, p. 79-87, 2014, http://acee-journal.pl/1,7,33,Issues.html [Dostęp: 01.06.2016]
20. J. Lelieveld, J. S. Evans, M. F. D. Giannadaki, and A. Pozzer. „The contribution of outdoor air pollution sources to premature mortality on a global scale." *Nature*, no. 525, p. 367-371, 2015, https://doi.org/10.1038/nature15371 [Dostęp: 05.03.2017].
21. U. Leopold, G. Huevelink, L. Drouet, and D. Zachary. „Modelling Spatial Uncertainties associated with Emission Disaggregation in an integrated Energy Air Quality Assessment Model," in IEMSs 2012 International Congress on Environmental Modelling and Software. Managing Resources of a Limited Planet: Pathways and Visions under Uncertainty, Sixth Biennial Meeting, S. L. R. Seppelt, A.A. Voinov and D. Bankamp, Eds., Leipzig, Germany, 2012, http://www.iemss.org/sites/iemss2012//proceedings-/D1_1_0823_Leopold_et_al.pdf [Dostęp: 09.02.2017].
22. S. Lyon, A. Lembo Jr., M. Todd Walter, and T. Steenhuis. „Defining probability of saturation with indicator kriging on hard and soft data." *Advances in Water Resources*, vol. 29, p. 181-193, 2006, https://doi.org/10.1016/j.advwatres.2005.02.012.
23. J. Maes, J. Vliegen, K. Van de Vel, S. Janssen, F. Deutsch, K. De Ridder, and C. Mensink. „Spatial surrogates for the disaggregation of CORINAIR emission inventories." *Atmospheric Environment*, vol. 43, no. 6, p. 1246-1254, 2009, https://doi.org/10.1016/j.atmosenv.2008.11.040 [Dostęp: 23.03.2017].
24. P. Marcotullio, A. Sarzynski, J. Albrecht, N. Schulz, and J. Garcia. "The geography of global urban greenhouse gas emissions: an exploratory analysis." Climatic Change, vol. 121, pp. 621-634, 2013, https://doi.org/10.1007/s10584-013-0977-z.
25. Q. Meng. „Spatial analysis of environment and population at risk of natural gas fracking in the state of Pennsylvania, USA." *Science of the Total Environment*, no. 515-516, p. 198-206, 2015, https://doi.org/10.1016/j.scitotenv.2015.02.030.

26. B. Namysłowska-Wilczyńska and A. Wilczyński. „Geostatistical Characteristics of the Structure of Spatial Variation of Electrical Power in the National 110KV Network Including Results of Variogram Model Components Filtering." *Acta Energetica*, no. 1/22, pp. 72-87, 2015, https://doi.org/10.12736/issn.2300-3022.2015106.
27. A. Nickless, R. Scholes, and E. Filby. „Spatial and temporal disaggregation of anthropogenic CO2 emisisons from the City of Cape Town." *South African Journal of Science*, vol. 111, pp. 1-8, 2015, https://doi.org/10.17159/sajs.2015/20140387.
28. W. Nikodem. „Rozważania nad kompleksową modernizacją systemu zaopatrzenia w ciepło Konurbacji Śląskiej." *Energetyka*, no. 5, pp. 381-388, 2008, [in Polish].
29. T. Oda and S. Maksyutov. „A very high-resolution (1km×1km) global fossil fuel CO2 emission inventory derived using a point source database and satellite observations of nighttime lights." *Atmos. Chem. Phys*., vol. 11, pp. 543-556, 2011, https://doi.org/-10.5194/acp-11-543-2011 [Dostęp: 16.05.2017].
30. R. Olea. „A six-step practical approach to semivariogram modeling." *Stoch Environ Res Risk Assess*, no. 20, pp. 307-318, 2006, https://doi.org/10.1007/s00477-005-0026-1 [Dostęp: 02.05.2017].
31. J. Ou, X. Liu, X. Li, and X. Shi. „Mapping Global Fossil Fuel Combustion CO2 Emissions at High Resolution by Integrating Nightlight, Population Density, and Traffic Network Data." *IEEE Journal of Selected Topics in Applied Earth Observations and Remote Sensing*, vol. 9, pp. 1674-1684, 2016, https://doi.org/10.1109/JSTARS.2015.2476347 [Dostęp: 23.05.2017].
32. M. Plebankiewicz and A. Jankowski. „Ciepło dla aglomeracji miast śląskich do wsparcia z funduszy unijnych." Wokół Energetyki, no. 3, pp. 1-4, 2007, http://www.cire.-pl/pliki/2/AGLOM.pdf. [in Polish].
33. M. Plejdrup, O.-K. Nielsen, and J. Brandt. „Spatial emission modelling for residential wood combustion in Denmark." Atmospheric Environment, vol. 144, pp. 389-396, 2016, https://doi.org/10.1016/j.atmosenv.2016.09.013.
34. L. Ran, D. Loughlin, D. Yang, Z. Adelman, B. Baek, and C. Nolte. „ESP v. 2.0: enhanced method for exploring emission impacts of future scenarios in the United States – addressing spatial allocation." Geoscientific Model Development, vol. 8, pp. 1775-1787, 2015, https://doi.org/10.5194/gmd-8-1775-2015 [Dostęp: 16.05.2017].
35. O. Schabenberger and C. Gotwa. *Statistical Methods for Spatial Data Analysis*. Chapman & Hall, 2004.
36. A. Soares. „Direct Sequential Simulation and Cosimulation." *Mathematical Geology*, vol. 33, no. 8, pp. 911-926, 2001, https://doi.org/10.1023/A:1012246006212.
37. P. Verburg, A. Tabeau, and E. Hatna. „Assessing spatial uncertainties of land allocation using a scenario approach and sensitivity analysis: A study for land use in Europe." *Journal of Environmental Management*, vol. 127, p. S132-S144, 2013, https://doi.org-/10.1016/j.jenvman.2012.08.038 [Dostęp: 25.04.2017].

38. Y. Wang and G. Li. „Mapping urban CO2 emissions using DMSP/OLS 'city lights' satellite data in China." Environment and Planning A, vol. 0, no. 0, pp. 1-4, 2016, https://doi.org/10.1177/0308518X16656374 [Dostęp: 02.03.2017].
39. J. Wu, W. Norvell, and R. Welch. „Kriging on highly skewed data for DTPA-extractable soil Zn with auxiliary information for pH and organic carbon." Geoderma, p. 187-199, 2006, https://doi.org/10.1016/j.geoderma.2005.11.002 [Dostęp: 12.01.2017].
40. H. Yu and A. Stuart. „Exposure and inequality for select urban air pollutants in the Tampa Bay area." *Science of the Total Environment*, vol. 551-552, p. 474-483, 2016, https://doi.org/10.1016/j.scitotenv.2016.01.157 [Dostęp: 12.02.2017].
41. E. Zajusz-Zubek, A. Mainka, Z. Korban, and J. Pastuszka. „Evaluation of highly mobile fraction of trace elements in PM10 collected in Upper Silesia (Poland): Preliminary results." *Atmospheric Pollution Research*, vol. 6, pp. 961-968, 2015, https://doi.org-/10.1016/j.apr.2015.05.001 [Dostęp: 05.04.2017].
42. J. Zawadzki. „Analiza rozkładu przestrzennego zanieczyszczenia gleb Warszawy i okolic cynkiem, miedzią i ołowiem z zastosowaniem krigingu wskaźnikowego." *Inżynieria i Ochrona Środowiska*, vol. 6, no. 3/4, pp. 407-424, 2003.
43. J. Zawadzki. *Metody geostatystyczne dla kierunków przyrodniczych i technicznych*. Warszawa, 2011.
44. Y. Zhao, L. Qiu, R. Xu, F. Xie, Q. Zhang, Y. Yu, C. Nielsen, H. Qin, H. Wang, X. Wu, W. Li, and J. Zhang. „Advantages of a city-scale emission inventory for urban air quality research and policy: the case of Nanjing, a typical industrial city in the Yangtze River Delta, China." Proceedings of the Federated Conference on Computer Science and Information Systems, vol. 15, p. 12623-12644, 2015, https://doi.org/10.5194/acp-15-12623-2015.
45. Y. Zhao, X. Xu, B. Huang, W. S. X. Shao, X. Shi, and X. Ruan. „Using robust kriging and sequential Gaussian simulation to delineate the copper- and lead-contaminated areas of a rapidly industrialized city in Yangtze River Delta, China." *Environmental Geology*, vol. 52, p. 1423-1433, 2007, https://doi.org/10.1007/s00254-007-0667-0.
46. B. Zheng, Q. Zhang, D. Tong, C. Chen, C. Hong, M. Li, G. Geng, Y. Lei, H. Huo, and K. He. „Resolution dependence of uncertainties in gridded emission inventories: a case study in Hebei, China." *Atmos. Chem. Phys*., vol. 17, p. 921-933, 2017, https://doi.org/-10.5194/acp-17-921-2017 [Dostęp: 05.03.2017].

SELECTED PROBLEMS OF EMISSION INVENTORIES – GEOSTATISTICAL PERSPECTIVE

Abstract: *This paper presents approach that develops currently applied methodology for obtaining spatial surrogates for spatial disaggregation of air emission inventories. Considered sector was small residential combustion in the Katowice Urban Zone, situated in the southern part of Poland, due to its importance in emission budget, also potential health threatening of the 'low emission' sector.Results presented in this paper use geostatistical techniques: ordinary and indicator kriging to show dependence between spatial distribution of the urban density development (described by the built areas) and distribution of the district heating infrastructure. Obtained results should be useful for emission inventory compilers, for air quality modelers as well as policymakers.*

Key words: *air emission inventory, spatial disaggregation, spatial allocation, air emission mapping geostatistics*

WYBRANE PROBLEMY INWENTARYZACJI EMISJI - PERSPEKTYWA GEOSTATYSTYCZNA

Streszczenie: *Niniejszy artykuł przedstawia wkład do rozwoju metodyki stosowanej do przestrzennego podziału inwentaryzacji emisji z udziałem tzw. surogatów. Zastosowanie krigingu zwykłego oraz wskaźnikowego jest zaprezentowane dla rozkładu przestrzennego obszarów zabudowanych, który jest surogatem emisji zanieczyszczeń do powietrza z gospodarstw domowych. Gospodarstwa domowe są ważnym źródłem sprzyjającym powstawaniu zjawiska tzw. „niskiej emisji" w Polsce. Wyniki przedstawiające zależność przestrzenną pomiędzy rozkładem przestrzennym obszarów zabudowanych, a rozkładem infrastruktury Śląskiego Systemu Ciepłowniczego. Mogą być wykorzystane do przygotowania lokalnych inwentaryzacji emisji na potrzeby modelowania jakości powietrza, a także dla rozwoju lokalnych polityk jakości powietrza.*

Słowa kluczowe: *inwentaryzacje emisji, dezagregacja przestrzenna, rozkłady przestrzenne, geostatystyka*

Mgr inż. Damian ZASINA
IEP-NRI, KOBiZE
ul. Chmielna 132/134, 00-805 Warszawa
e-mail: damian.zasina@kobize.pl

Prof. dr hab. Jarosław ZAWADZKI
Warsaw University of Technology
Faculty of Building Services, Hydro
and Environmental Engineering
ul. Nowowiejska 20, 00-653 Warszawa
e-mail: J.J.Zawadzki@gmail.com

Data przesłania artykułu do Redakcji: 15.05.2017
Data akceptacji artykułu przez Redakcję: 11.06.2017